Accepted Manuscript

Title: Surface properties of distinct nanofibrillated celluloses assessed by inverse gas chromatography

Author: José A.F. Gamelas Jorge Pedrosa Ana F. Lourenço Paulo J. Ferreira

PII: S0927-7757(15)00002-3
DOI: http://dx.doi.org/doi:10.1016/j.colsurfa.2014.12.058
Reference: COLSUA 19639

To appear in: *Colloids and Surfaces A: Physicochem. Eng. Aspects*

Received date: 29-10-2014
Revised date: 9-12-2014
Accepted date: 30-12-2014

Please cite this article as: J.A.F. Gamelas, J. Pedrosa, A.F. Lourenço, P.J. Ferreira, Surface properties of distinct nanofibrillated celluloses assessed by inverse gas chromatography, *Colloids and Surfaces A: Physicochemical and Engineering Aspects* (2015), http://dx.doi.org/10.1016/j.colsurfa.2014.12.058

Surface properties of distinct nanofibrillated celluloses assessed by inverse gas chromatography

José A.F. Gamelas*, Jorge Pedrosa, Ana F. Lourenço, Paulo J. Ferreira

Department of Chemical Engineering, CIEPQPF, University of Coimbra, Pólo II – R. Silvio Lima, 3030-790 Coimbra, Portugal. *jafgas@eq.uc.pt.

Highlights:

- Nanocelluloses were distinguished from each other for their surface properties
- Dispersion component of the surface energy (γ_s^d) at 40 ºC was of 42-52 mJm^{-2}
- Higher γ_s^d value was found for enzymatic nanocellulose than for TEMPO-oxidised ones
- For TEMPO-nanocelluloses acidity/basicity ratio increased with the fibrillation
- Results may have interest in the composites production area/coatings applications

Abstract

The adhesion and surface properties of nanocelluloses are an important issue to consider when using this material for composites production, in food packaging or coatings, as well as for determining the influence of added functional groups. In the present work, the surface properties of two nanofibrillated celluloses obtained by mild 2,2,6,6-tetramethylpiperidine-1-oxyl radical (TEMPO)-mediated oxidation with distinct mechanical treatment intensity in a homogenizer (5 and 15 passes), and one nanofibrillated cellulose obtained by enzymatic process, were thoroughly assessed by inverse chromatography, at infinite dilution conditions. The dispersion component of the surface energy (γ_s^d) was 42-46 mJ m^{-2} at 40 ºC for the TEMPO nanofibres and 52 mJ m^{-2} for the enzymatic nanocellulose. It was confirmed, based on the determination of the specific components of the works of adhesion and enthalpies of adsorption with polar probes, that the surfaces of the materials have a more Lewis acidic than

Lewis basic character. Regarding TEMPO nanofibres, a slight increase of Lewis acidity/basicity ratio seemed to occur for the more nanofibrillated material (15-passes). Higher specific interactions with polar probes were found for enzymatic nanocellulose. The higher values of γ_s^d and specific interactions observed for the enzymatic nanocellulose could partly be due to the higher crystallinity of this sample. On the other hand, the increase of the acidity/basicity ratio (as well as of the γ_s^d value) for the 15-passes vs. 5-passes TEMPO nanofibres was attributed to a higher exposition of the hydroxyl groups of cellulose at the surface of the former material.

Keywords: composites, inverse gas chromatography, nanocellulose, surface energy, Lewis acid-base character

Introduction

Nanofibrillated cellulose (NFC) is a type of cellulose fibres with nanosized diameters (typically in the range of 15-60 nm) and lengths up to several micrometers, being sometimes also referred to as microfibrillated cellulose (MFC). It is usually obtained from bleached kraft pulp or non-woody materials by a homogenization process under high pressure, which may be preceded by a chemical pre-treatment. The chemical pre-treatments are used to decrease the energy needed for fibrillation and can be of several types, namely enzymatic, 2,2,6,6-tetramethylpiperidine-1-oxyl radical (TEMPO)-mediated oxidation pre-treatment, carboxymethylation and acetylation processes. The chemical pre-treatment with NaClO (oxidant) and TEMPO and NaBr as catalysts at pH 10-11 is by far the most commonly employed. Using this pre-treatment, the C6 hydroxyl groups of cellulose are converted to aldehyde and carboxylate groups, which enable the nanofibrils within the fibres to separate better from each other due to the repulsive forces between the ionized carboxylic acids [1].

NFC possesses several properties that make it a potential interesting material for a wide range of applications. Amongst its more relevant properties are the relatively high specific surface area in comparison to that of the pristine cellulose fibres (values can be higher than 100 m^2/g), the viscosity (rheology) properties of the viscous NFC gel, the high tensile strength and the high light transmittance of the corresponding NFC films. NFC has thus been used in formulations as a viscosity modifier, as gel for biomedical applications, as a mechanical reinforcement material in (nano)composites, including (nano)paper, for paper coating, in films for food packaging and for electronic devices [2-8]. Its barrier properties namely for the water vapour and molecular oxygen have been highlighted [1].

The adhesion and surface properties of nanocellulose are key points that have to be considered regarding the aforementioned uses, for instance, in composites or in barrier materials [1, 9-10]. Studies on the surface properties of nanofibres have been generally focused on i) the determination of "surface" charge by zeta potential measurements or by polyelectrolyte titration, ii) the determination of the amount of carboxylate and aldehyde groups formed during chemical pre-treatments, by conductometric and potentiometric titrations and, iii), the assessment of the chemical composition and reactivity of the nanocellulose surface during chemical pre-treatments/surface modification, by using X-ray photoelectron spectroscopy [1,10].

One powerful tool to assess the surface properties of solid materials is inverse gas chromatography (IGC). It enables to obtain the dispersion component of the surface energy, adsorption thermodynamic parameters with a wide range of polar substances (specific components of the free energy of adsorption, enthalpy and entropy of adsorption), Lewis acid-base character of the surface, surface nanoroughness parameter, etc. [11-14]. Thus, using IGC a cellulosic fibrous material can be thoroughly characterized with respect to its surface chemical properties. Besides, this technique is advantageous over the classical contact angle

measurements for the analysis of porous, rough, heterogeneous and hydrophilic surfaces. Not many papers reported the use of IGC to analyse nanocellulose [15-19]. In particular, under infinite dilution conditions, the dispersion component of the surface energy was determined for cellulose nanofibers obtained by enzymatic pre-treatments [15] and cellulose nanofibers extracted from hemp fibre by acid hydrolysis [16]. For the latter, the Lewis acid-base characteristics were also assessed. The influence of the drying method on the surface energy of cellulose nanofibrils was also evaluated [18].

In the present work, two nanofibrillated celluloses obtained from an eucalypt bleached kraft pulp, by NaClO/TEMPO/NaBr pre-oxidation with distinct mechanical treatment intensity, and one nanofibrillated cellulose obtained by enzymatic process, were thoroughly analysed for their surface properties by inverse chromatography. The results of these analyses with regard to a wide range of assessed parameters will be presented and discussed.

Experimental

TEMPO-oxidised cellulose nanofibres were obtained by firstly treating a bleached eucalypt pulp with NaClO (4 mmol/g of pulp) and catalytic amounts of TEMPO and NaBr, accordingly to a previously reported methodology [20]. The fibres were then passed through a homogeneizer (GEA Niro Soavi Panda Plus 2000) 5 times at 300 bar or 15 times (five passes at 300 bar and 10 passes at 600 bar), affording NFC-5p and NFC-15p, respectively. The enzymatic nanocellulose was purchased from Grenoble INP-Pagora. This sample was obtained from a softwood bisulfite pulp by treatment with endoglucanases followed by homogenization with 1 pass at 1000 bar and 4 passes at 1500 bar. The nanofibres suspensions were characterized for their general properties, as described below.

The suspensions were then freeze-dried and milled in order to obtain a solid material that was then packed into the IGC column for the physico-chemical surface analysis.

In order to evaluate the relative amount of nanofibrillar material in each original sample, the transmittance of NFC suspensions (0.1%, w/w) in the 400-800 nm visible range was measured using a Jascow V550 spectrophotometer. Besides, 40 ml of each NFC suspension, previously diluted up to 0.2% w/w, was centrifuged at 4500 rpm for 20 min, and the retained fraction was analyzed for its solid content and compared to the original to obtain by difference the percentage (w/w) of supernatant material. The results were an average of three replicated measurements. To evaluate the nanofibres "surface" charge, zeta potential measurements were carried out in triplicate in a Zetasizer Nano ZS from Malvern Instruments.

The inverse gas chromatography analysis was performed using a DANI GC 1000 digital pressure control gas chromatograph equipped with a hydrogen flame ionization detector. Stainless-steel columns, 0.5 m long and 0.4 cm inside diameter were washed with acetone and dried before packing. For each analysis, approximately 1 g of nanocellulose was packed into the gas chromatograph column. The columns were shaped in a smooth ''U" to fit the detector/injector geometry of the instrument. The packed columns were conditioned overnight at 105 ºC, under a helium flow (P=0.1 bar), before any measurements were made. Measurements were carried out at four different temperatures (40, 45, 50 and 55 ºC) with the injector and detector kept at 180ºC and 200ºC, respectively. Helium was used as carrier gas. Small quantities of probe vapor (<1 μL) were injected into the carrier gas, allowing work under infinite dilution conditions. The probes used for the IGC data collection were *n*-pentane (C5), *n*-hexane (C6), *n*-heptane (C7), *n*-octane (C8), *n*-nonane (C9), trichloromethane (TCM, Lewis acidic probe), tetrahydrofurane (THF, basic), ethyl acetate (ETA, amphoteric) and acetone (amphoteric). It should be noted that polar probes with similar molecular surface area

values and different electron donating/acceptor properties were chosen, in order to assess only the effect of Lewis acid-base interactions with the materials surface. All probes were of chromatographic grade and were used as received (Sigma–Aldrich). Methane was used as the reference probe. The retention times were the average of three injections and were determined by the peak maximum for the *n*-alkanes and TCM or by the Conder and Young method for THF, ETA and acetone, which provided less symmetrical chromatograms [21]. The coefficient of variation between runs was typically lower than 3%. Two columns were prepared for each material with the final results being the average of two separate measurement series. The theoretical aspects of inverse gas chromatography have been previously described [11-13]. Using this technique, the dispersion component of the surface energy, and the specific components of the work of adhesion, enthalpy and entropy of adsorption of polar probes on the surface of the analysed materials were obtained. The values of the molecular surface area (a) and dispersion component of the surface energy (γ^d) of the probes used for the IGC analysis can be found elsewhere [11-12].

Additionally, the crystallinity of the freeze-dried NFCs was assessed using X-ray diffraction. X-ray diffraction data were collected in a Philips X'Pert diffractometer operating in the Bragg-Brentano configuration with Co-kα (λ=1.79 Å) source at a current of 35 mA and an accelerating voltage of 40 kV. Data were collected by the step counting method (step 0.025º and time 1.0 s) in the 2θ range of 5-50º. The crystallinity was determined by the Segal method as $(I_{Cr}-I_{am})/I_{cr}*100$, where I_{cr} refers to the intensity of the reflection from the 002 plane at about 26º and I_{am} is the intensity of the amorphous halo between the reflection around 19º and the reflection from the 002 plane [22]. There are other methods for determination of crystallinity based on the X-ray diffraction peaks area or using other techniques such as solid-state ^{13}C NMR [23]. For the purposes of the present study, *i.e.*, to differentiate TEMPO and enzymatic cellulose nanofibres, the Segal method is appropriate.

FTIR-ATR spectra were obtained using a Jasco FT/IR-4200 spectrometer. The spectra were recorded in the 500–4000 cm^{-1} range with a resolution of 4 cm^{-1} and a number of scans of 64.

Results and discussion

The percentage of fibrillar material separated at the supernatant by centrifugation, determined as described in the experimental section and noted as "yield", as well as the zeta potential and transmittance results are shown in Table 1. The zeta potential values of NFC-5p and NFC-15p are negative and similar, in agreement with the presence of ionized carboxylic acids at the surface of nanofibres generated during the oxidative pre-treatment with NaClO/TEMPO/NaBr. On the other hand, a low negative value was obtained for enzymatic nanocellulose, corresponding to an unstable colloidal dispersion. With regard to the yield, a very low value was obtained for the enzymatic nanocellulose. This is essentially a consequence of the easy aggregation and sedimentation of enzymatic nanofibres, because their zeta potential is close to zero. Thus, during the centrifugation of the enzymatic nanocellulose suspension, most of the nanofibres do not remain in the supernatant but, instead, deposit in the form of aggregates, and for this reason, a low yield value is obtained. The values for NFC-5p and NFC-15p were significantly higher and the highest was the one of the NFC-15p sample (95%), as expected due to the more extensive mechanical treatment. The visible spectra of the NFC suspensions in the transmittance mode (Fig. 1) confirmed the different relative amount of nanofibres/aggregation degree of nanofibres in the materials suspensions, that is, for the TEMPO-oxidised celluloses a higher amount of nanosized material (15-passes vs. 5-passes) provides a clearer dispersion thus giving a higher

transmittance. For the enzymatic nanocellulose the high aggregation degree of nanofibres yields a very low transmittance.

Please, insert Table 1

Please, insert Figure 1

The dispersion component of the surface energy (γ_s^d) at 40 ºC of the studied nanocelluloses was in the range of 42-52 mJ m^{-2} and was found to increase in the following order: NFC-5p < NFC-15p < enzymatic nanocellulose (Table 2). The values here obtained for the TEMPO nanocelluloses are comparable to that previously reported, at infinite dilution conditions, for cellulose nanofibers extracted from hemp fibre by acid hydrolysis and mechanical treatment (42 mJ m^{-2}) [16]. However, the γ_s^d value found here for the enzymatic nanocellulose was significantly higher than those reported in a previous study for cellulose nanofibres also obtained by enzymatic pre-treatments (γ_s^d values at 40 ºC of 37–45 mJ m^{-2}) [15]. On the other hand, significantly higher values have been obtained for bacterial cellulose (61 mJ m^{-2}) [17].

Please, insert Table 2

The slight increase of γ_s^d from NFC-5p to NFC-15p can be related to the aforementioned increase of the fibrillation, since a more nanofibrillated material will have a larger number of hydroxyl groups, which are considered to have a major contribution to the dispersion component of the surface energy of cellulose [18,25], accessible on the surface for interaction with the IGC apolar probes. The differences in the γ_s^d values between the TEMPO-oxidised nanocelluloses and the enzymatic nanocellulose can partly be due to the different crystallinity of the nanocelullose samples. It has been proposed previously that more crystalline celluloses show a higher surface energy [26,27]. In particular, bacterial cellulose nanocrystals samples, possessing a high crystallinity index, showed γ_s^d values higher than 60 mJ m^{-2} [17,19]. In

order to confirm this hypothesis, X-ray diffractograms of the NFC-15p and enzymatic nanocellulose samples were recorded. As shown in Figure 2, the crystallinity of the enzymatic nanocellulose was much higher than that of NFC-15p (see the intensity of the reflection peaks relatively to the amorphous halo), being estimated a crystallinity index of 79% for enzymatic nanocellulose and of 65% for NFC-15p. Thus, the higher crystallinity of the enzymatic nanocellulose can be, at least partially, responsible for the higher dispersion component of the surface energy observed for this sample. Other impurities present at the NFCs surface, not analysed in the present study, will also have an influence on the surface energy. These results confirm the influence of the nature of treatment used for obtaining the nanocelluloses on their surface energy. Besides, and as usually reported for cellulosic materials [16,28], a decreasing trend of the γ_s^d value with temperature for the several nanocelluloses types was found (Figure 3).

Please, insert Figure 2

Please, insert Figure 3

The Lewis acid-base characteristics of the nanocelluloses surfaces were assessed firstly based on the calculation of the specific component of the work of adhesion (W_a^s) of several polar probes (Figure 4 and Table 2). The results indicate that the nanocelluloses surfaces have significantly higher affinity for Lewis amphoteric (acetone, ETA) and basic (THF) probes than for acidic (TCM) probe. Similar conclusions can be held for the $-\Delta G_a^s$ values, because these are related to the works of adhesion by $-\Delta G_a^s = N.a.W_a^s$ (N is the Avogadro number) and the molecular surface area values of the used polar probes are similar, thus giving similar trends (not presented in Table 2 for a matter of simplicity). The acidic surface character is mainly due to the presence of acidic hydroxyl groups in the cellulose structure [25, 28-30]. For NFC-5p and NFC-15p, the carboxylate groups formed during the oxidative pre-treatment of cellulose should have a minor contribution to the Lewis acidity, since they are mostly in

the ionized (COO^-) form and not in the protonated (COOH, acidic) one (note that the analysed freeze-dried samples were obtained from NFC aqueous suspensions at pH around 7). This was confirmed by measuring the FTIR-ATR spectra of the NFC samples. In fact, the spectra of the TEMPO-oxidised cellulose nanofibres showed in the 1500-1800 cm^{-1} region a band at 1605 cm^{-1} due to the CO stretching of the ionized form of the acid [31], in addition to a shoulder at ca. 1640 cm^{-1} due to the OH bending of absorbed water; the characteristic carboxylic acid band at 1720-1730 cm^{-1} [31] was not detected (Figure 5). For the enzymatic nanocellulose only the OH bending vibration of water was observed (Figure 5).

A slight increase of the W_a^s(THF)/W_a^s(TCM) ratio (Table 2) was observed from NFC-5p to NFC-15p probably due to a higher exposition of the acidic groups at the surface of NFC-15p, as a consequence of the higher fibrillation of the latter material. Accordingly, the W_a^s values with amphoteric probes also increased for NFC-15p.

Please, insert Figure 4

Please, insert Figure 5

Following a trend similar to that of the γ_s^d values, higher W_a^s values were obtained for the enzymatic nanocellulose. The substitution of a few hydroxyl groups for carboxylate groups (COO^- Na^+) in the TEMPO NFCs would generate, in principle, a reduction of the Lewis acidity and an increase of the Lewis basicity of the material because hydroxyl is mainly an electron acceptor (acidic) group while COO^- is mainly an electron donor (basic) group. In fact, the TEMPO NFCs showed lower specific affinities with THF (basic probe) and with acetone and ETA (amphoteric probes with more Lewis basic than Lewis acidic character [11-12]) than the enzymatic nanocellulose. However, the affinity with an acidic probe such as TCM was not higher for the TEMPO NFCs. This indicates that other factors must also be considered in order to understand the differences in the magnitude of the specific interactions of polar probes on the nanofibres surface. As demonstrated above by X-ray diffraction, the enzymatic nanocellulose is much more crystalline than the NFC-15p (Fig. 2). Thus, it is

probable that the overall higher specific interactions observed with the enzymatic nanocellulose, in comparison to those with the TEMPO NFCs, can also be due to the higher crystallinity of the former (higher crystallinity affords stronger intermolecular interactions) [19]. It should be noted that previously Siddiqui et al. [15] used IGC to obtain the γ_s^d value of an enzymatic nanocellulose but could not measure the magnitude of the interaction with polar probes (due to the low amount of packed material). Overall, the specific interactions results indicate that the treatment used to produce enzymatic nanocellulose can render the surface even more Lewis polar than the surface of NFCs obtained by TEMPO-mediated oxidation, in terms of the highest-energy sites assessed by IGC.

The specific component of the enthalpy and entropy of adsorption, ΔH_a^s and ΔS_a^s, respectively, of each polar probe on the nanocelluloses surface were also evaluated from the plots of $\Delta G_a^s/T$ versus $1/T$ at four different temperatures (40, 45, 50 and 55 ºC). As a consequence of the poor linear fittings/very low correlations of $\Delta G_a^s/T$ versus $1/T$ obtained for enzymatic nanocellulose (r values lower than 0.8), no ΔH_a^s and ΔS_a^s acceptable data are presented for this material. It should be noted that the ΔH_a^s and ΔS_a^s results are dependent on a large number of retention time measurements, carried out at several temperatures, and in these circumstances propagated errors can have a greater influence on the final results.

The results of ΔH_a^s and ΔS_a^s for NFC-5p and NFC-15p (Table 3) confirmed the higher interactions with the amphoteric and basic probes, as demonstrated *e.g.*, by the ΔH_a^s(THF)/ΔH_a^s(TCM) ratio. When comparing the two TEMPO nanofibrillated celluloses it is noted that both the specific enthalpic ($-\Delta H_a^s$) and entropic ($-\Delta S_a^s$) terms for the adsorption of polar probes are typically lower with NFC-15p. The resulting specific components of the free energy of adsorption ($-\Delta G_a^s$) or the related specific components of the work of adhesion (Table 2) were higher for the more nanofibrillated cellulose, because $-\Delta G_a^s = -\Delta H_a^s - T.(-\Delta S_a^s)$. Thus, in what respects the Gibbs free energy of adsorption and the corresponding

entropic contribution, the adsorption of polar probes is more favoured for NFC-15p, although the opposite trend is revealed by the enthalpic term comparison. In addition, there was an increase of the ΔH_a^s(THF)/ΔH_a^s(TCM) enthalpic ratio from NFC-5p to NFC-15p, in accordance with the trend observed for the aforementioned W_a^s(THF)/W_a^s(TCM) ratio.

Please, insert Table 3

Overall, the results of the specific interactions with Lewis acidic (TCM) and basic (THF) probes, namely the W_a^s, $-\Delta G_a^s$ and $-\Delta H_a^s$ values, suggested that all the studied NFCs have a more Lewis acidic than Lewis basic character. Previously, it has been reported, based on the determination of the Lewis acidity (K_a) and basicity (K_b) constants, that hemp cellulose nanocrystals [16] and cellulose nanofibrils after different drying methods [18] were more basic than acidic ($K_b > K_a$) .We may note that the straight comparison of the K_a values with the K_b values should be made with due caution, as previously discussed [12 and references therein]. The comparison of the magnitude of specific interactions with different probes may be more appropriate to assess the Lewis acid-base character of the material surface.

Conclusions

Inverse gas chromatography (IGC) enabled to evaluate the surface properties of nanocelluloses obtained by different methods, namely by a pre-treatment with NaClO/TEMPO/NaBr and by an enzymatic process. Two TEMPO-oxidised samples, obtained using a mild chemical pre-treatment (4 mmol NaClO/g pulp) but a different intensity of mechanical treatment in a homogenizer (5- and 15-passes), were considered.

The dispersion component of the surface energy was in the range of 42-52 mJ m^{-2} (at 40 ºC), being obtained a higher value for enzymatic nanocellulose. TEMPO-oxidised nanofibres

obtained after 15-passes in a homogenizer also showed a higher γ_s^d value than those obtained after 5 passes. Concerning the specific interactions with polar probes, they were always of higher magnitude with the amphoteric and basic probes, as measured by the specific components of the works of adhesion and enthalpies of adsorption. The highest specific interactions were found for enzymatic nanocellulose. For the TEMPO-oxidised nanofibres, a slight increase of acidity/basicity ratio seemed to occur with the increase of the intensity of the applied mechanical treatment. Overall, the behaviour of nanocelluloses was not much different from that expected for cellulose molecules but some differences between the samples surfaces were clearly revealed by the calculation of the surface energy parameters, using IGC at infinite dilution conditions.

References

[1] N. Lavoine, I. Desloges, A. Dufresne, J. Bras, Microfibrillated celulose – its barrier properties and applications in cellulosic materials: a review, Carbohydr. Polym. 90 (2012) 735-764.

[2] S. Ahola, M. Österberg, J. Laine, Cellulose nanofibrils – adsorption with poly(amideamine) epichlorohydrin studied by QCM-D and application as a paper strength additive, Cellulose 15 (2008) 303–314.

[3] C. Aulin, M. Gällstedt, T. Lindström, Oxygen and oil barrier properties of microfibrillated cellulose films and coatings, Cellulose 17 (2010) 559–574.

[4] F.W Brodin, O.W. Gregersen, K. Syverud, Cellulose nanofibrils: Challenges and possibilities a paper additive or coating material, Nord. Pulp Paper Res. J. 29 (2014) 156-166.

[5] G. Chinga-Carrasco, D. Tobjörk, R. Österbacka, Inkjet-printed silver-nanoparticles on nano-engineered cellulose films for electrically conducting structures and organic transistors – concept and challenges. J. Nanopart. Res. 14 (2012) 1213.

[6] M.H.J. Korhonen, J. Laine, Flocculation and retention of fillers with nanocelluloses, Nord. Pulp Paper Res. J. 29 (2014) 119-128.

[7] D.V. Plackett, K. Letchford, J.K. Jackson, H.M. Burt, A review of nanocellulose as a novel vehicle for drug delivery, Nord. Pulp Paper Res. J. 29 (2014) 105-118.

[8] K. Syverud, P. Stenius, Strength and permeability of MFC films, Cellulose 16 (2009) 75-85.

[9] D.J.Gardner, G.S. Oporto, R. Mills, M.A.S.A. Samir, Adhesion and surface issues in cellulose and nanocellulose, J Adhes. Sci. Technol. 22 (2008) 545–567.

[10] H. Kangas, P. Lahtinen, A. Sneck, A-M. Saariaho, O. Laitinen, E. Hellén, Characterization of fibrillated celluloses. A short review and evaluation of characteristics with a combination of methods, Nord. Pulp Paper Res. J. 29 (2014) 129-143.

[11] J.M.R.C.A. Santos, J.T. Guthrie, Analysis of interactions in multicomponent polymeric systems: the key-role of inverse gas chromatography, Mat. Sci. Eng. R. 50 (2005) 79–107.

[12] J.A.F. Gamelas, The surface properties of cellulose and lignocellulosic materials assessed by inverse gas chromatography: a review, Cellulose 20 (2013) 2675-2693.

[13] P. Mukhopadhyay, H.P. Schreiber, Aspects of acid-base interactions and use of inverse gas chromatography, Colloids Surf. A 100 (1995) 47–71.

[14] J.A.F. Gamelas, E. Ferraz, F. Rocha, An insight into the surface properties of calcined kaolinitic clays: The grinding effect, Colloids Surf. A 455 (2014) 49-57.

[15] N. Siddiqui, R.H. Mills, D.J. Gardner, D. Bousfield, Production and characterization of cellulose nanofibers from wood pulp, J. Adhes. Sci. Technol. 25 (2011) 709–721.

[16] B. Wang, M. Sain, The effect of chemically coated nanofiber reinforcement on biopolymer based nanocomposites, Bioresources 2 (2007) 371–388.

[17] M. Pommet, J. Juntaro, J.Y.Y. Heng, A. Mantalaris, A.F. Lee, K. Wilson, G. Kalinka, M.S.P. Shaffer, A. Bismarck, Surface modification of natural fibers using bacteria: depositing

bacterial cellulose onto natural fibers to create hierarchical fiber reinforced nanocomposites, Biomacromolecules 9 (2008) 1643–1651.

[18] Y. Peng, D.J. Gardner, Y. Han, Z. Cai, M.A. Tshabalala, Influence of drying method on the surface energy of cellulose nanofibrils determined by inverse gas chromatography, J Colloid Interface Sci. 405 (2013) 85-95.

[19] I.A. Sacui, R.C. Nieuwendaal, D.J. Burnett, S.J. Stranick, M. Jorfi, C. Weder, E.J. Foster, R.T. Olsson, J.W. Gilman, Comparison of the properties of cellulose nanocrystals and cellulose nanofibrils isolated from bacteria, tunicate, and wood processed using acid, enzymatic, mechanical, and oxidative methods, ACS Appl. Mater. Interfaces 6 (2014) 6127-6138.

[20] T. Saito, S. Kimura, Y. Nishiyama, A. Isogai, Cellulose nanofibres prepared by TEMPO-mediated oxidation of native cellulose, Biomacromolecules 8 (2007) 2485-2491.

[21] D.P. Kamdem, B. Riedl, Inverse gas chromatography of lignocellulosic fibers coated with a thermosetting polymer: use of peak maximum and conder and young methods, J. Colloid Interface Sci. 150 (1992) 507–516.

[22] L. Segal, J.J. Creely, A.E. Martin, C.M. Conrad, An empirical method for estimating the degree of crystallinity of native cellulose using the X-ray diffractometer, Textile Res J. 29 (1959) 786–94.

[23] A.D. French, M.S. Cintrón, Cellulose polymorphy, crystallite size, and the Segal crystallinity index, Cellulose 20 (2013) 583-588.

[24] J. Schultz, L. Lavielle, C. Martin, The role of the interface in carbon fibre-epoxy composites, J. Adhesion 23 (1987) 45–60.

[25] G. Garnier, W.G. Glasser, Measuring the surface energies of spherical cellulose beads by inverse gas chromatography, Polym. Eng. Sci. 36 (1996) 885–894.

[26] M.N. Belgacem, A. Blayo, A. Gandini, Surface characterization of polysaccharides, lignins, printing ink pigments, and ink fillers by inverse gas chromatography, J Colloid Interface Sci. 182 (1996) 431–436.

[27] E. Papirer, E. Brendle, H. Balard, C. Vergelati, Inverse gas chromatography investigation of the surface properties of cellulose, J. Adhes. Sci. Technol. 14 (2000) 321–337.

[28] M.G. Carvalho, J.M.R.C.A. Santos, A.A. Martins, M.M. Figueiredo, The effects of beating, web forming and sizing on the surface energy of *Eucalyptus globulus* kraft fibres evaluated by inverse gas chromatography, Cellulose 12 (2005) 371-383.

[29] J.M. Felix, P. Gatenholm, H.P. Schreiber, Controlled interactions in cellulose-polymer composites. 1. Effect on mechanical properties. Polym. Compos. 14 (1993) 449–457.

[30] M.A. Tshabalala, Determination of the acid-base characteristics of lignocellulosic surfaces by inverse gas chromatography, J. Appl. Polym. Sci .65 (1997) 1013–1020.

[31] C. Schutz, J. Sort, Z. Bacsik, V. Oliynyk, E. Pellicer, A. Fall, L. Wagberg, L. Berglund, L. Bergstrom, G. Salazar-Alvarez, Hard and transparent films formed by nanocellulose–TiO_2 nanoparticle hybrids, PLoS One 7 (2012) e45828.

Figure captions

Fig. 1. Visible spectra in the transmittance mode of 0.1% suspensions of NFC-5p, NFC-15p and enzymatic nanocellulose.

Fig. 2. X-ray diffractograms of NFC-15p and enzymatic nanocellulose.

Fig. 3. γ_s^d values at several temperatures for NFC-5p, NFC-15p and enzymatic nanocellulose.

Fig. 4. Plots of $RT\ln(V_n)$ vs. $2N \cdot a(\gamma_l^d)^{0.5}$ for NFC-5p, NFC-15p and enzymatic nanocellulose at 40 ºC.

Fig. 5. FTIR-ATR spectra of NFC-15p and enzymatic nanocellulose (see the highlighted region).

Note: old Figs 1 and 6 were removed.

Table 1. Results on the production of cellulose nanofibres by TEMPO-mediated oxidation and enzymatic process

Material	Zeta Potential (mV)	Yield (%)[a]	Transmittance (600 nm, %)
NFC-5p	-41±4	63±3	23
NFC-15p	-46±3	95±1	56
Enzym NFC	-12±2	8±1	5

[a] Determined as the percentage of supernatant material relative to the original sample after centrifugation at 4500 rpm for 20 min

Table 2. Dispersion component of the surface energy (γ_s^d, mJ m^{-2}) and specific component of the work of adhesion (W_a^s, mJ m^{-2}) of polar probes for TEMPO-oxidised cellulose nanofibres and enzymatic nanocellulose[a]

Material	γ_s^d	W_a^s (TCM)	W_a^s (THF)	W_a^s (acetone)	W_a^s (ETA)	W_a^s(THF)/ W_a^s(TCM)
NFC-5p	41.7±0.4	5.2±0.6	21.7±0.1	28.0±0.6	23.5±0.3	4.2
NFC-15p	46.2±2.4	4.4±0.2	23.4±0.5	32.1±0.3	25.8±0.5	5.4
Enzym NFC	51.5±0.8	6.2±0.2	26.9±0.6	36.9±0.5	28.5±0.1	4.4

[a]Values at 40 ºC calculated following Schultz and Lavielle approach [24].

Table 3. Specific components of the enthalpy and entropy of adsorption for TEMPO-oxidised cellulose nanofibres[a]

Material	Probe	$-\Delta H_a^s$ ($x10^6$, mJ/mol)	$-\Delta S_a^s$ ($x10^4$, mJ/mol)	$-\Delta H_s$ (THF)/ $-\Delta H_s$ (TCM)
NFC-5p				
	TCM	8.9±1.7	2.4±0.6	2.2
	THF	19.0±2.8	4.2±0.9	
	Acetone	19.5±0.5	3.9±0.2	
	ETA	22.6±4.5	5.1±1.4	
NFC-15p				
	TCM	5.2±2.3	1.3±0.8	2.8
	THF	13.9±2.7	2.4±0.8	
	Acetone	15.9±1.9	2.4±0.6	
	ETA	12.6±0.1	1.6±0.01	

[a]from measurements in the 40-55 ºC range. Correlation coefficients for the linear plots of $\Delta G_a^s/T$ versus $1/T$ were in the range of 0.95-1.00.

Fig. 2

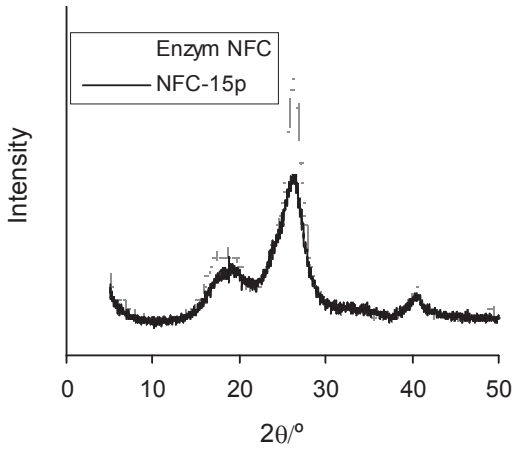

Fig. 3

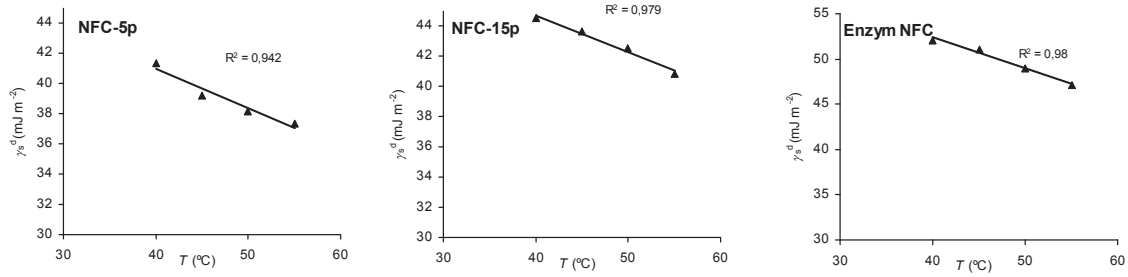

Fig. 4

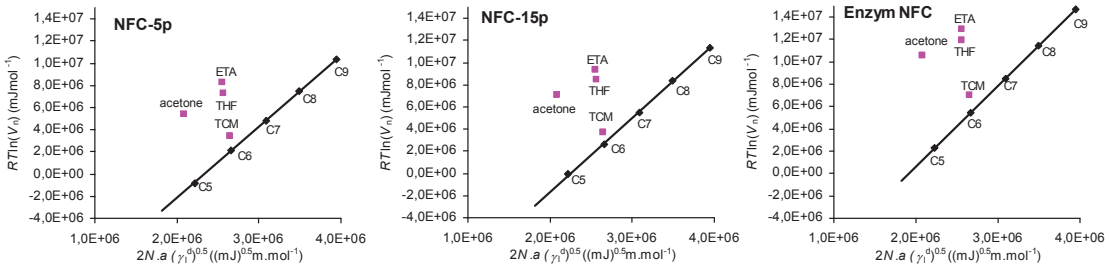

Figure 5

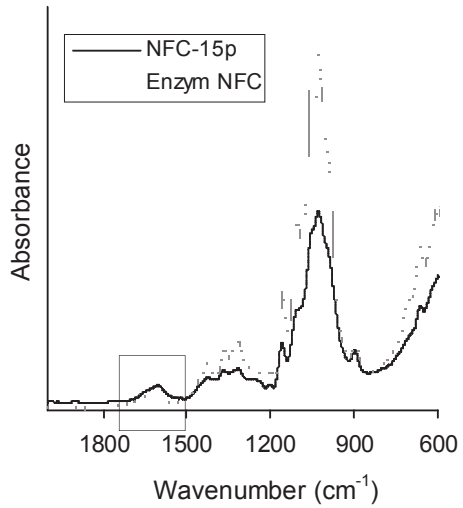

Fig. 1

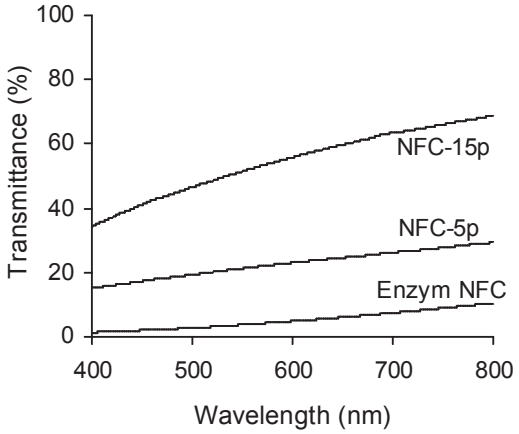

Cellulose nanofibres

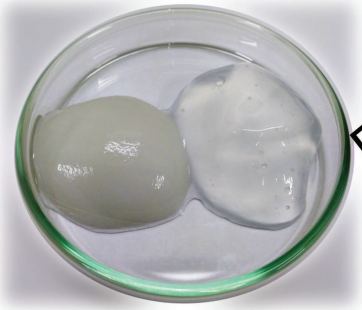

Freeze-drying

IGC